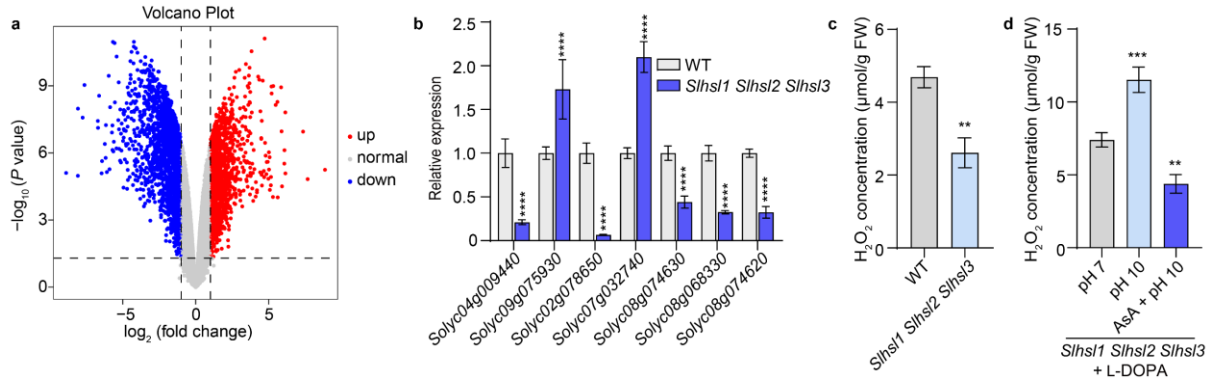


**Supplementary Fig. S1 RNA-seq analysis of the AZ in *Slhsl1 Slhsl2 Slhsl3* and WT plants and $H_2O_2$ concentrations**

**a**, Volcano plot showing the numbers of downregulated (blue) and upregulated (red) differentially expressed genes in the AZs of *Slhsl1 Slhsl2 Slhsl3* relative to WT plants at 8 h after flower removal, as determined by RNA-seq. **b**, RT-qPCR validation of the relative expression levels of seven DEGs identified by RNA-seq in the AZs of WT and *Slhsl1 Slhsl2 Slhsl3*. Data are shown as means ± standard deviation (SD; $n$ = 3). **c**, **d**, $H_2O_2$ concentration in the AZs of WT and *Slhsl1 Slhsl2 Slhsl3* plants at 8 h after flower removal (**c**) and in the AZs of *Slhsl1 Slhsl2 Slhsl3* treated with L-DOPA at pH 7.0, pH 10.0, or pH 10.0 + ascorbic acid (AsA) (**d**). Data are shown as means ± SD ($n$ = 3). Statistical analysis: two-way analysis of variance (ANOVA) with Šidák's multiple comparison test (**b**); unpaired two-tailed $t$-test (**c**); one-way ANOVA with Dunnett's test (**d**). Significance levels: **, $P < 0.001$; ***, $P < 0.0001$; ****, $P < 0.00001$.

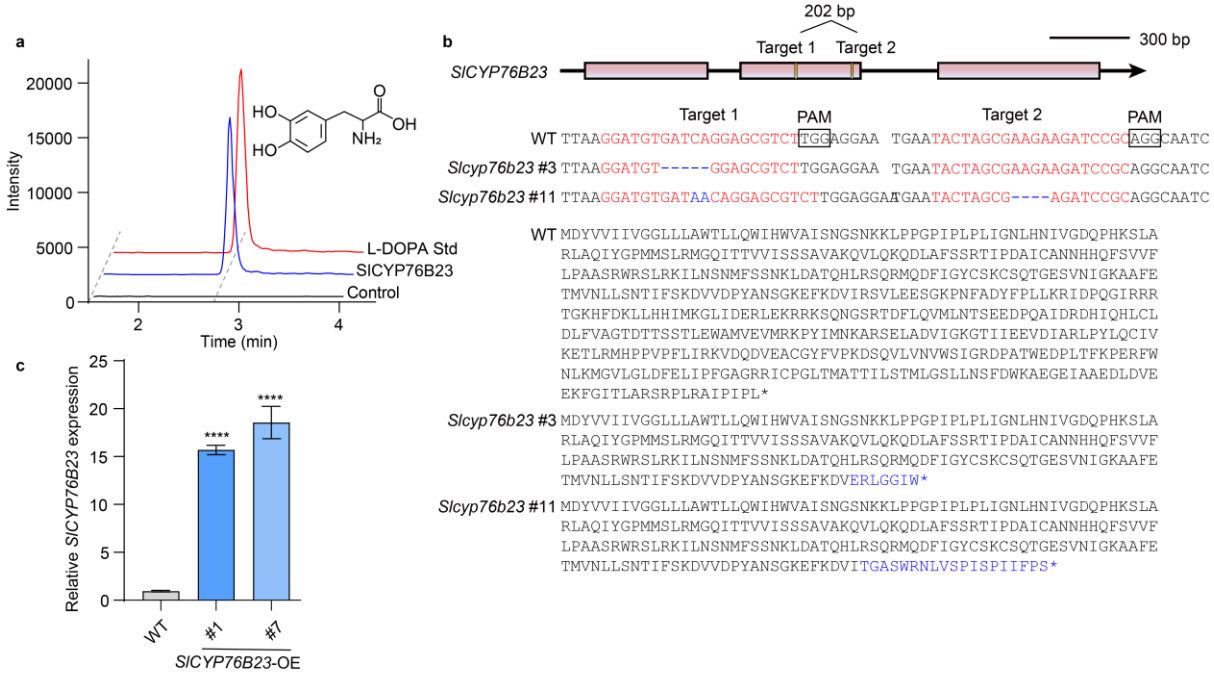


**Supplementary Fig. S2 Enzymatic activity of SlCYP76B23, knockout, and overexpression of *SlCYP76B23***

**a**, Enzymatic activity assay for SlCYP76B23. Heterologous expression of *SlCYP76B23* in yeast strain BY4742 and subsequent HPLC–MS/MS assay demonstrating its catalytic conversion of L-tyrosine to L-DOPA; the empty vector was used as a control. **b**, CRISPR/Cas9-mediated editing of *SlCYP76B23*. Diagram of the *SlCYP76B23* genomic locus and the target sites for the two single guide RNAs (sgRNAs). Red sequences denote sgRNA target sites, and black boxes indicate the protospacer-adjacent motifs (PAMs). Blue dashes and letters represent deletions and insertions, respectively. All identified alleles are predicted to result in premature termination of translation. **c**,

Relative *SlCYP76B23* expression levels in WT and *SlCYP76B23*-overexpressing (OE) lines as determined by RT-qPCR. Data are shown as means ± SD ($n$ = 3). Statistical analysis: one-way ANOVA with Dunnett's multiple comparison test (**c**). Significance level: ****, $P < 0.0001$.

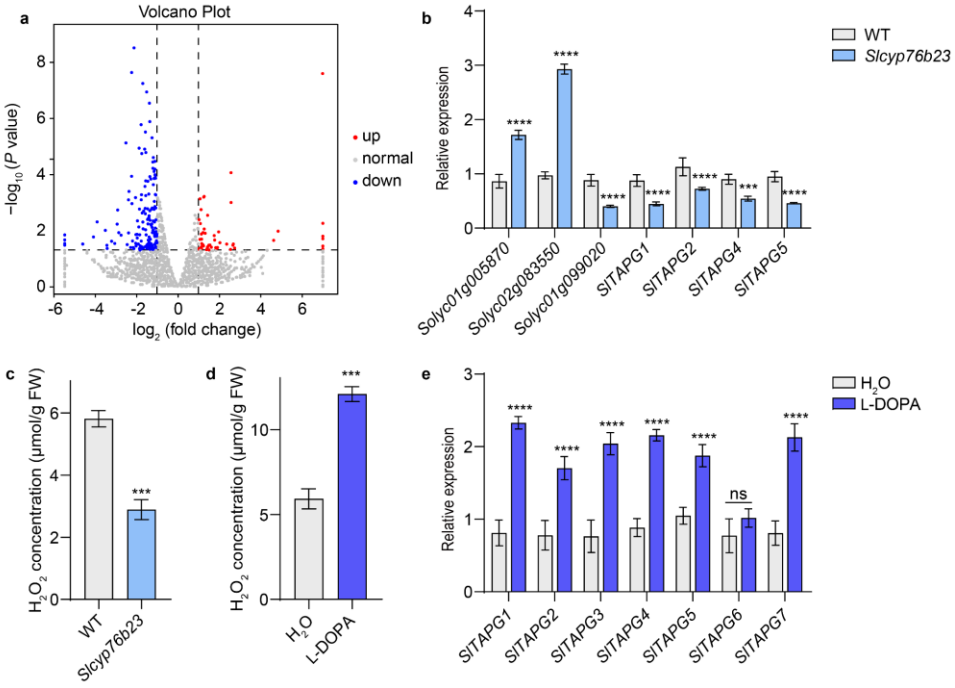


**Supplementary Fig. S3 RNA-seq analysis of AZs in *Slcyp76b23* and WT plants, $H_2O_2$ concentrations, and *SlTAPGs* expression**

**a**, Volcano plot showing the DEGs in the AZs of *Slcyp76b23* relative to WT plants at 8 h after flower removal. Blue and red dots indicate downregulated and upregulated genes, respectively, as determined by RNA-seq. **b**, RT-qPCR validation of expression levels for seven DEGs identified by RNA-seq in the AZs of *Slcyp76b23* and WT plants. Data are shown as means ± SD ($n$ = 3). **c**, **d**, $H_2O_2$ concentration in the AZs of WT and *Slcyp76b23* at 8 h after flower removal (**c**) and in the AZs of WT treated with or without L-DOPA (**d**). Data are shown as means ± SD ($n$ = 3). **e**, Relative *SlTAPG1–7* transcript levels in the AZs of WT flower pedicels after 8 h of treatment with or without L-DOPA treatment. Relative expression was quantified by RT-qPCR. Data are shown as means ± SD ($n$ = 3). Statistical analysis: two-way ANOVA with Šidák's multiple comparison test (**b**, **e**); unpaired two-tailed $t$-test (**c**, **d**). Significance level: ns, not significant; ***, $P < 0.001$; ****, $P < 0.0001$.

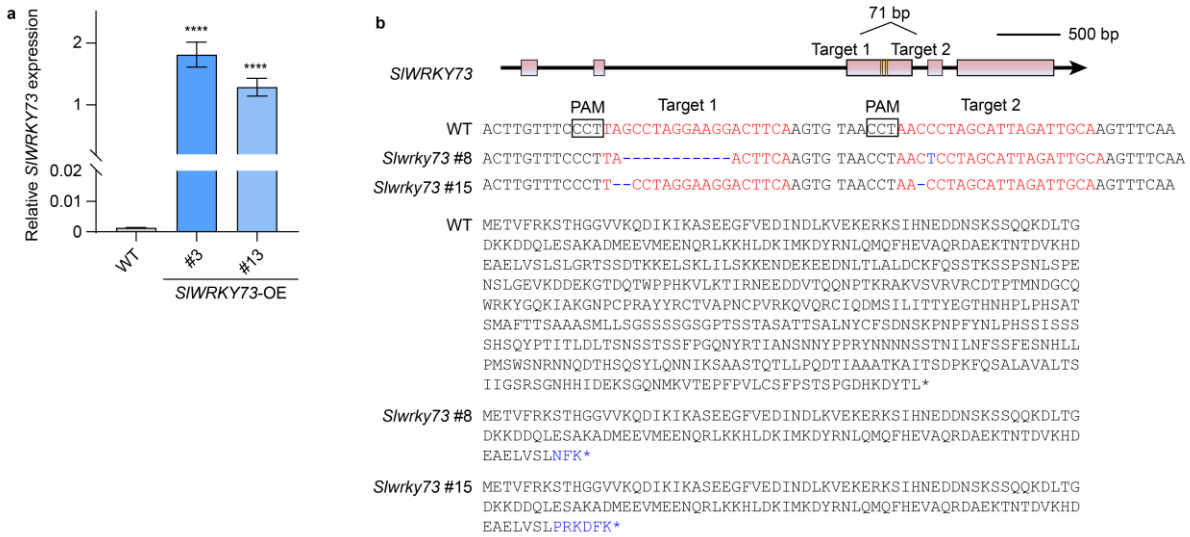

**Supplementary Fig. S4 *SlWRKY73* overexpression and knockout lines**

**a**, Relative *SlWRKY73* expression levels in WT and *SlWRKY73*-OE lines as determined by RT-qPCR. Data are shown as means ± SD ($n$ = 3). **b**, CRISPR/Cas9-mediated editing of *SlWRKY73*. Diagram of the *SlWRKY73* genomic locus showing the positions of the two sgRNAs used to induce mutations. Red sequences denote sgRNA target sites, and black boxes indicate PAMs. Blue dashes and letters represent deletions and insertions, respectively. Statistical analysis: one-way ANOVA with Dunnett's multiple comparison test (**a**). Significance level: ****$P$ < 0.0001.

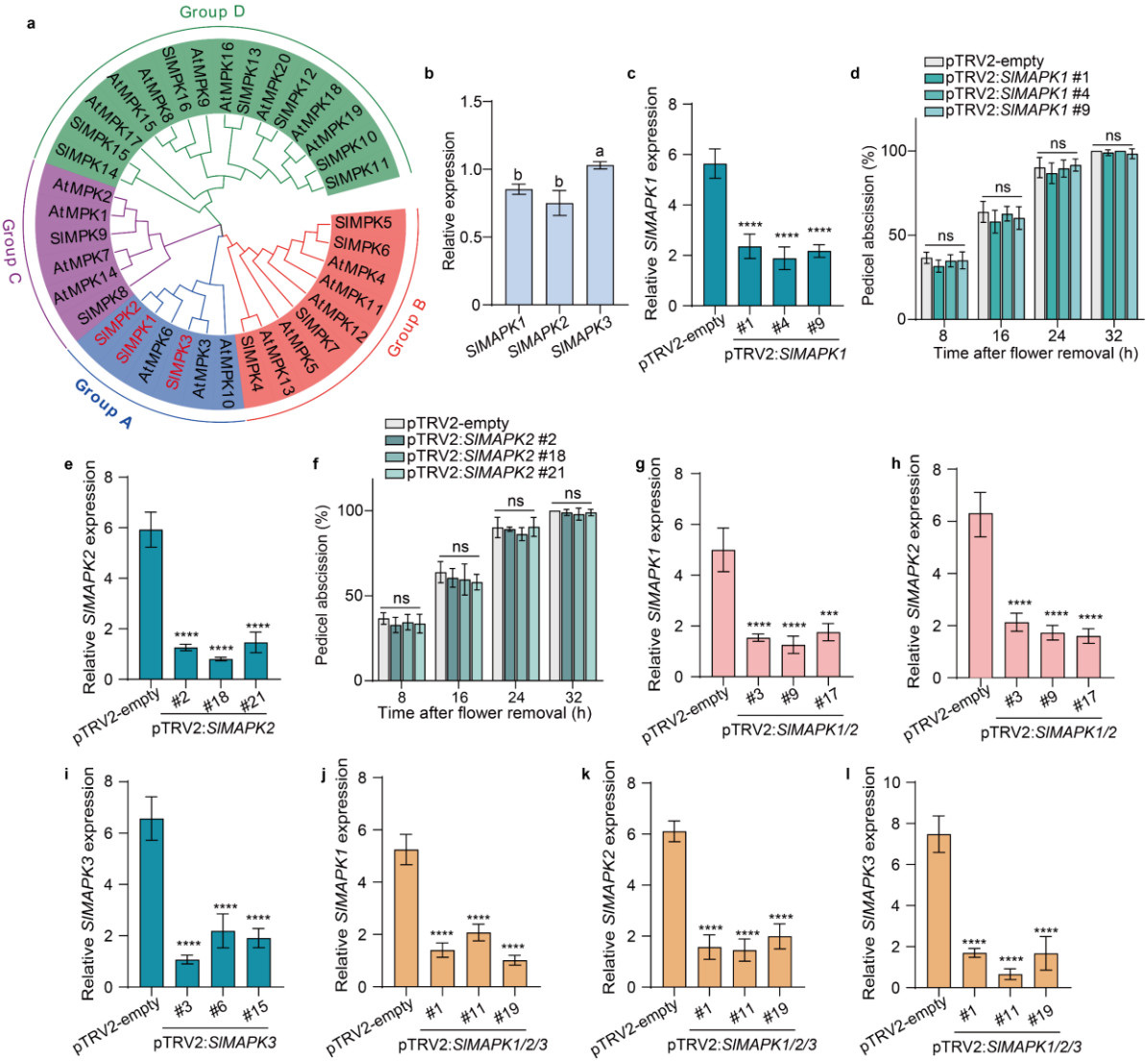


**Supplementary Fig. S5 Characteristics, silencing efficiency of *MAPK*s, and abscission phenotypes of MAPKs**

**a**, Phylogenetic analysis of AtMAPKs and SlMAPKs using the neighbor-joining method in MEGA7. **b**, Relative transcript levels of *SlMAPK1–3* in the AZs of WT plants at 8 h after flower removal. Data are shown as means ± SD ($n$ = 3). **c**, Relative *SlMAPK1* transcript levels in the AZs of pTRV2-empty and pTRV2:*SlMAPK1* plants. Data are shown as means ± SD ($n$ = 3). **d**, Abscission rates of pTRV2-empty and pTRV2:*SlMAPK1* plants. Data are shown as means ± SD ($n$ = 3). **e**, Relative *SlMAPK2* transcript levels in the AZs of pTRV2-empty and pTRV2:*SlMAPK2* plants. Data are shown as means ± SD ($n$ = 3). **f**, Abscission rates of pTRV2-empty and pTRV2:*SlMAPK2* plants. Data are shown as means ± SD ($n$ = 3). **g**, **h**, Relative transcript levels of *SlMAPK1* (**g**) and *SlMAPK2* (**h**) in the AZs of pTRV2-empty and pTRV2:*SlMAPK1/2* plants. Data are shown as means ± SD ($n$ = 3). **i**, Relative *SlMAPK3* transcript levels in the AZs of pTRV2-empty and pTRV2:*SlMAPK3* plants. Data are

shown as means ± SD ($n$ = 3). **j**–**l**, Relative transcript levels of *SlMAPK1* (**j**), *SlMAPK2* (**k**), and *SlMAPK3* (**l**) in the AZs of pTRV2-empty and pTRV2:*SlMAPK1/2/3* plants. Data are shown as means ± SD ($n$ = 3). Statistical analysis: one-way ANOVA with Tukey's multiple comparison test (**b**); one-way ANOVA with Dunnett's test (**c**, **e**, **g**–**l**); two-way ANOVA with Tukey's test (**d**, **f**). Significance levels: ns, not significant; ***, $P < 0.001$; ****, $P < 0.0001$; different lowercase letters indicate significant differences at $P < 0.05$.

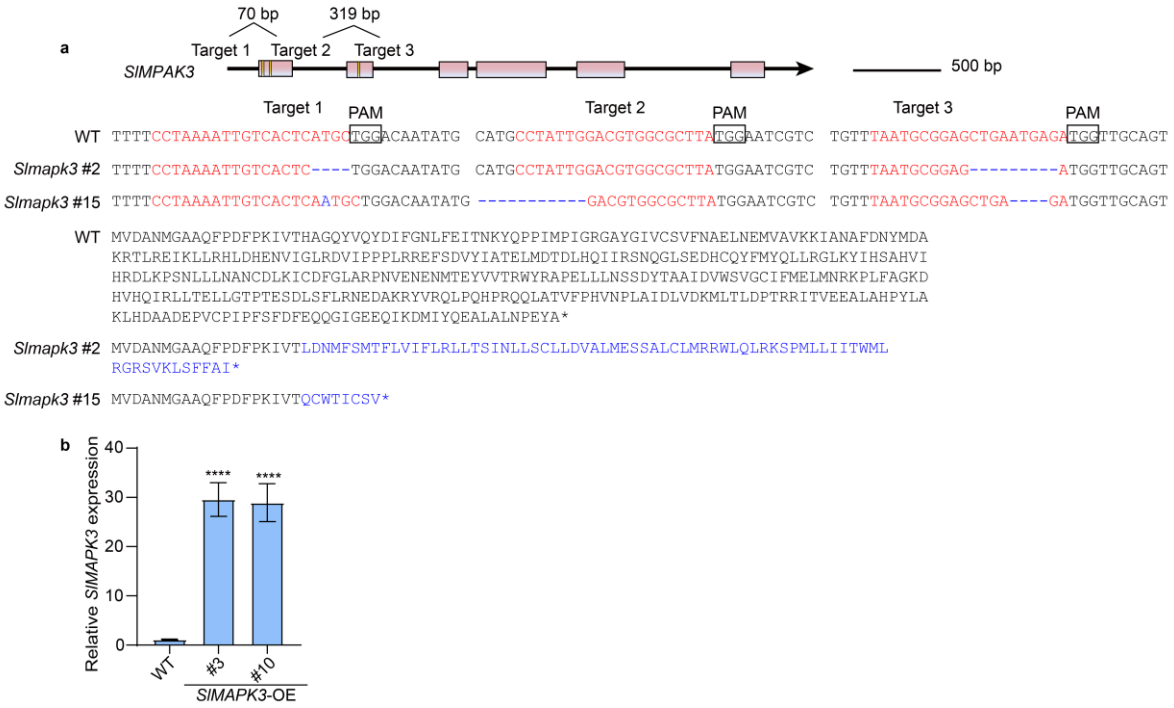


**Supplementary Fig. S6 Identification of *SlMAPK3* knockout and overexpression lines**

**a**, CRISPR/Cas9-mediated editing of *SlMAPK3*. Diagram of the *SlMAPK3* genomic locus showing the positions of the three sgRNAs used to induce mutations. Red sequences denote sgRNA target sites, and black boxes indicate PAMs. Blue dashes and letters represent deletions and insertions, respectively. **b**, Relative *SlMAPK3* expression levels in WT and *SlMAPK3*-OE lines as determined by RT-qPCR. Data are shown as means ± SD ($n$ = 3). Statistical analysis: one-way ANOVA with Dunnett's multiple comparison test (**b**). Significance levels: ****, $P < 0.0001$.

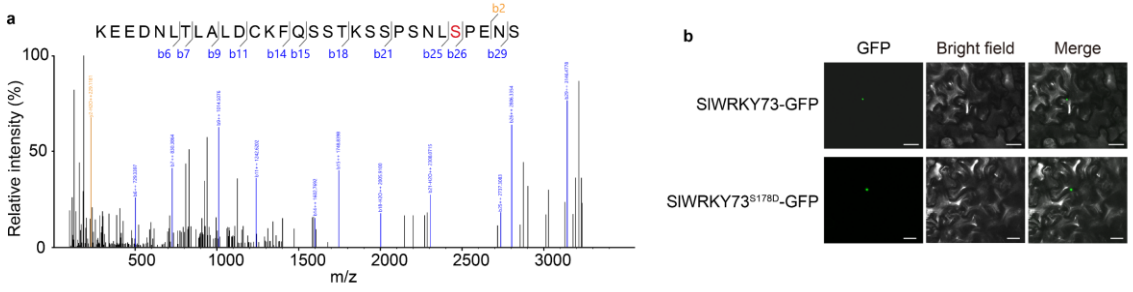


**Supplementary Fig. S7 Mapping the phosphorylation site and subcellular localization of SlWRKY73.**

**a**, Phosphorylation site mapping of SlWRKY73 by LC–MS/MS. Red letters indicate phosphorylated residues. **b**, Subcellular localization assays in *N. benthamiana* leaves revealing that SlMAPK3-mediated phosphorylation of SlWRKY73 does not affect its nuclear localization. *N. benthamiana* leaves were infiltrated with *35S:SlWRKY73-GFP* or *35S:SlWRKY73*$^{S178D}$*-GFP*. Scale bars, 25 μm.